Proceedings of the
47th IEEE Conference on Decision and Control
Cancun, Mexico, Dec. 9-11, 2008

TuA14.4

On the effect of communication constraints on robust performance for a practical 802.15.4 Wireless Sensor Network Benchmark problem

Michael J. Walsh, S. M. Mahdi Alavi and Martin J. Hayes

Abstract— This work considers the effect of communication constraints on the dynamic performance of wireless sensor networks that operate in a power aware mode. In particular, the hardware output power limit and quantization constraints that arise practically when only a limited number of power levels are available to the designer are considered in this regard. A novel approach is presented that uses an intuitively appealing graphical means of representing an output power constraint, whereby the saturation block that naturally occurs in a practical setting is mapped from the output of the plant and is compensated through the use of a robust Anti-Windup scheme. System performance and stability is verified using quantitative feedback theory in the linear part of the design. The hybrid controller that ensues is extensively tested experimentally, on a fully compliant 802.15.4 testbed, where mobility is considered in the problem formulation using a team of fully autonomous robots. A benchmark comparison is made between this approach and a number of existing strategies suggesting that an anti-windup approach is an entirely appropriate methodology for the problem at hand.

I. INTRODUCTION

Wireless sensor networks (WSNs) consist of inexpensive miniature devices capable of computation, communication and sensing. By replacing a wired communications network, they provide the ability to observe physical phenomena at a fine resolution over large spatio-temporal scales. The application space is quite large and is continually growing, encompassing habitat, ecosystem, seismic and industrial process monitoring, security and surveillance as well as rapid emergency response and wellness maintenance.

It has been shown in [1] that 70% of the energy consumed by widely available embedded WSN platforms is as a result of data transmission. It therefore stands to reason that transmission power control for WSNs is a worthwhile endeavor. To achieve this, some measure of performance or quality of service must be readily available to the designer. One such link estimator is the received signal strength indicator (RSSI). Until recently it was assumed that RSSI was a poor indication of link quality. However it is now understood [2] that this assumption was founded on experimentation with early platforms equipped with older radios, e.g. the CC1000, where hardware miscalibration was quite a common phenomenon. Newer, more sophisticated transceiver radios, such as the CC2420, have significantly reduced this problem and it has also been shown [2], that RSSI exhibits a very small variation over time when its value is above the sensitivity threshold.

The authors are with the Wireless Access Research Center, ECE Department, University of Limerick, Limerick, Ireland `michael.j.walsh@ul.ie`, `mahdi.s.alavi@ul.ie`, `martin.j.hayes@ul.ie`

Other work [1] has established a solid relationship between RSSI and signal to noise plus interference ratio (SINR). This relationship is exploited here to guarantee pre-specified performance objectives in terms of packet error rate (PER) as outlined in [3]. Using RSSI as a feedback metric and adjusting the transmitter power accordingly can therefore be used as a means of managing wireless channel performance.

There are a number of aspects that must be considered when choosing which control algorithm to implement. One key and often overlooked issue is the limited power capabilities of each mobile node. Several schemes model the adverse effects generated by these constraints as noise [4] or assume the system will achieve the performance objectives without surpassing power output limitations [5]. However the presence of these saturation limits can severely degrade network performance and could possibly lead to instability if not properly addressed.

It is the authors' opinion that the problem lies in the position of the saturation nonlinearity at the output of the system. While there have been some advances in control design theory to deal with output constraints [6], there is a vast literature covering the treatment of linear systems subject to input saturation constraints [7]. One solution therefore lies in the mapping of the output saturation constraint to the input of the plant or the output of the controller. Using this approach allows for a more conservative controller design approach guaranteeing graceful performance degradation in the face of the nonlinearity. The systems science concept of Anti-Windup (AW) is extremely useful in this regard. This work practically implements an intuitively appealing two step AW design procedure on an 802.15.4 compliant wireless sensor testbed. The first step is to design a linear controller ignoring the inherent nonlinear constraints on the system. The control design approach adopted here is based on quantitative feedback theory and provides both robust stability and nominal performance in the linear operational region. The second step involves using recent advances in AW theory, to minimize degradation in the face of actuator constraints. The technique employed here is known as Weston -Postlethwaite Anti-Windup (WP-AW) Synthesis. First presented in [8] and later in its discrete-ized form in [9], this technique uses an $\mathcal{L}_2$ approach in conjunction with linear matrix inequality (LMI) optimization techniques to ensure that during saturation the systems performance remains close to nominal linear operation and returns to the linear operational region as quickly as possible.

(a)

(b)
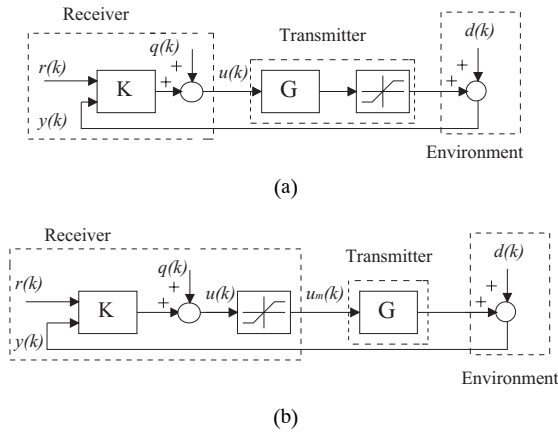
Fig. 1. Wireless System Model with (a) Saturation block at the output, (b) Saturation block mapped from output to input.

II. PROBLEM DEFINITION

A. The saturation function

The saturation function is defined as

$$sat(u) := [sat_1(u_1), ..., sat_m(u_m)], \quad (1)$$

where $sat_i(u_i) := sign(U_i) \times min\{|u_i|, \bar{u}_i\}$, with $\bar{u}_i > 0$ is the ith saturation limit. The following set is defined

$$\mathcal{U} := [-\bar{u}_1, \bar{u}_1] \times, ..., \times [-\bar{u}_m, \bar{u}_m], \quad (2)$$

where clearly $sat(u) = u$, $\forall u \in \mathcal{U}$. This is the set in which the saturation behaves linearly. This set can be mapped directly from the output of a system to its input as will be shown later.

B. The Network Model

The system shown in figure 1(a) has output $y(k)$ (RSSI), controller output $u(k)$ (power level), and reference input $r(k)$ (reference RSSI). $q(k)$ is quantization noise associate with switching between power levels. The plant $G(z)$ is represented by $G(z) = [G_1(z) \ G_2(z)]$, where $G_1(z)$ and $G_2(z)$ are the disturbance feedforward and feedback parts of $G(z)$ respectively. $d(k)$ is a disturbance to the system and comprises of channel attenuation, interference and noise. Given no disturbance model is available in the form of a transfer function, $G_1(z)$ is taken to be $G_1 = I$ where I is the identity matrix. The controller $K(z)$ takes the form $K(z) = [K_1(z) \ K_2(z)]$ a standard two degree of freedom structure. Figure 1(b) portrays the system with the saturation block mapped from the output of the system to the input where $u_m(k)$ is the saturated input to the plant. To represent the mapped saturation function we define the new set

$$\mathcal{U}_n := [-\bar{u}_1/h_{G_2}, \bar{u}_1/h_{G_2}] \times, ..., \times [-\bar{u}_m/h_{G_2}, \bar{u}_m/h_{G_2}], \quad (3)$$

where h_{G_2} is the gain of the transfer function G_2, selected as a low pass filter with sufficient bandwidth to eliminate quantization noise. $G_2(z)$ is determined to be

$$G_2(z) = \frac{1}{1.1z - 0.9}. \quad (4)$$

As mentioned previously we use a similar approach to [1] to directly estimate the SINR using the RSSI. This allows us to select a setpoint or reference RSSI value and relate it directly to PER as outlined in the 802.15.4 standard [3]. To expand, the bit error rate (BER) for the 802.15.4 standard operating at a frequency of 2.4GHz is given by

$$BER = \frac{8}{15} \times \frac{1}{16} \times \sum_{k=2}^{16} -1^k \begin{pmatrix} 16 \\ k \end{pmatrix} e^{20 \times SINR \times (\frac{1}{k} - 1)}, \quad (5)$$

and given the average packet length for this standard is 22 bytes, the PER can be obtained from

$$PER = 1 - (1 - BER)^{PL} \quad (6)$$

where PL is packet length including the header and payload. Establishing a relationship between RSSI, SINR and subsequently PER can therefore help to pre-specify levels of system performance. From [1] the SINR is given by:

$$\gamma(k) \approx RSSI(k) - n(k) - C - 30 \quad (7)$$

where the addition of the scalar term 30 accounts for the conversion from dBm to dB, $n(k)$ is thermal noise and C is the measurement offset assumed to be 45 dB.

III. ROBUST POWER TRACKING CONTROLLER DESIGN

The first step in the controller design procedure requires a linear controller design stage that ignores the control input nonlinearity. A design process that incorporates the Quantitative Feedback Theory of Horowitz [10] is adopted for this purpose. Consider the canonical form illustrated in figure 1(b). Initially the compensator, $K_2(z)$, is designed to attenuate the undesirable effects of uncertainty, disturbance and noise on the system. Having arrived at an appropriate $K_2(z)$, a pre-filter $K_1(z)$, is then designed so as to shift the closed-loop response to the desired tracking region specified *a priori* by the engineer. A set of desired specifications is subsequently introduced in terms of the magnitude of the frequency response of the closed-loop system so as to achieve robust stability *and* performance.

A. The desired specifications

In this paradigm, the notion of robust stability is usually incorporated into gain and phase margins through the use of the following constraint:

$$\left| \frac{K_2 G_2}{1 + K_2 G_2}(z) \right|_{z = e^{j\omega T_s}} \leq \mu, \quad (8)$$
$$for \ all \ G_2 \in \{\mathcal{G}\}, \omega \in [0, \pi/T_s].$$

Where $T_s = 3(sec)$, and the (nominal) plant G_2 is given by (4), as discussed in section 2. This criterion corresponds to lower bounds on the gain margin of $K_M = 1 + 1/\mu$ and the phase margin angle of $\phi_M = 180° - \cos^{-1}(0.5/\mu^2 - 1)$, [11]. Throughout the design, we adopt $\mu = 1.5$ thereby guaranteeing a phase and gain margin equal to $50°$ and 1.44, respectively.

(a) Feedback compensator design   (b) Pre-filter design
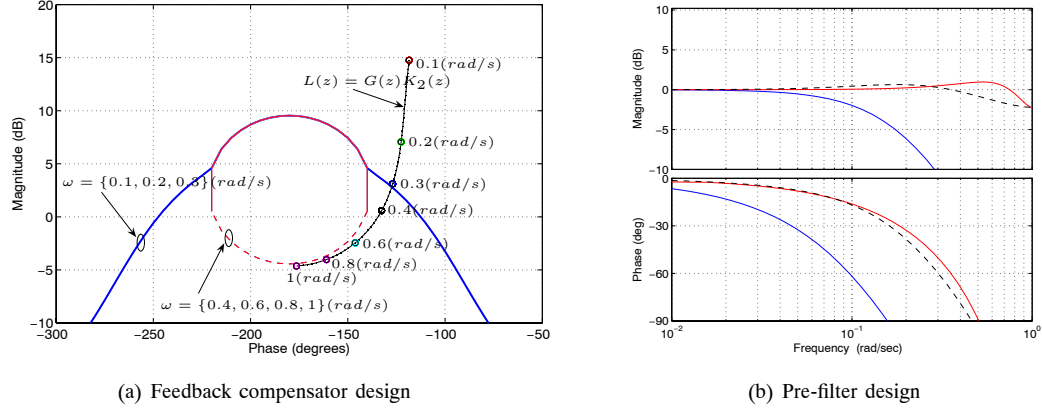
Fig. 2. QFT controllers. All design bounds are satisfied by $K_2(z)$, and $K_1(z)$.

The following design constraint is used to ensure adequate tracking performance,

$$|T_L(j\omega)| \le \left| \frac{K_2 G_2}{1 + K_2 G_2}(z) \right|_{z = e^{j\omega T_s}} \le |T_U(j\omega)|, \quad (9)$$
$$for\ all\ G_2 \in \{\mathcal{G}\}, \omega \in [0, \omega_h].$$

where ω_h denotes desired performance bandwidth. Equation (9) implies that the system RSSI should be placed in a pre-defined region specified by upper and lower bounds $T_U(z)$ and $T_L(z)$, respectively. $T_U(z)$ and $T_L(z)$ are typically defined by the engineer using time-domain concepts such as settling time and overshoot, [11]. Supposing that *i)* the RSSI should be required to settle around the target value of $5 \le t_{ss} \le 25(s)$, and *ii)* damping factor $\xi = 0.5$, is desired to reduce outage probability at the outset of communication, the following transfer functions can be selected so as to achieve the desired tracking bounds:

$$T_U(z) = \frac{0.9945z + 0.3891}{z^2 + 0.2928z + 0.09072} \quad (10)$$

$$T_L(z) = \frac{0.1219z + 0.08167}{z^2 - 1.098z + 0.3012} \quad (11)$$

It is necessary to attenuate the effects of link uncertainties and multiple user interference treated here as a disturbance. To achieve this, it is sufficient to over-bound the transfer function from $\overline{D}_i(k)$ to $\overline{r}_i(k)$ with an appropriate disturbance rejection ratio as follows:

$$\left| \frac{1}{1 + K_2 G_2}(z) \right| \le |W_D(z)|, \quad (12)$$
$$z = e^{j\omega T_s}\ for\ all\ G_2 \in \{\mathcal{G}\}, \omega \in [0, \omega_h].$$

where W_D represents a weighting function on the required levels of disturbance rejection. There must always be a trade off between stability and disturbance attenuation that has to be taken into consideration in the selection of W_D. Sweeping W_D from 0.1 to 1 demonstrates that $W_D = 0.9$ provides a reasonable disturbance attenuation ratio and produces a feasible controller that appropriately makes the trade-off.

Based on the desired tracking upper and lower bounds,

performance bandwidth is selected as $\omega_h = 0.3(rad/s)$.

B. Feedback compensator design

Using the MATLAB QFT-Toolbox [11], The design bounds associated with equation (8) and (12) are computed for $\{0.05, 0.1, 0.2, 0.3, 0.4, 0.5, 0.6, 0.7, 0.8, 0.9, 1\}\ (rad/s)$, and $\{0.05, 0.1, 0.2, 0.3\}\ (rad/s)$ respectively. The intersection of the bounds at each design frequency is the final bound taken for the design of the feedback compensator, $K_2(z)$. Figure 2(a) shows the obtained QFT design bounds. $K_2(z)$ is designed by adding appropriate poles and zeros to the loop function so that the nominal loop function frequency response satisfies the worst case design specification for the bounds at each frequency. For robustness, the nominal loop function must be shaped such that the frequency response lies above the design bounds at each design frequency and does not enter the U-contours described in figure 2(a). Moreover the critical point $(-180°, 0dB)$ must also be avoided.

Figure 2(a), illustrates that (13) satisfies the design bounds:

$$K_2(z) = \frac{z - 0.6622}{0.7103z - 0.7103} \quad (13)$$

C. Pre-filter design

The closed-loop transfer function is shaped by using $K_1(z)$ to place the system frequency response between two pre-defined lower and upper bounds, [10], [11]. Figure 2(b) shows that by using the following pre-filter, the closed-loop transfer function will place between $T_L(z)$ and $T_U(z)$. (14) satisfies the design bounds:

$$K_1(z) = \frac{1.4127z}{z - 0.4127} \quad (14)$$

IV. WESTON-POSTLETHWAITE ANTI-WINDUP (WP-AW) SYNTHESIS

The disturbance feedforward and feedback parts of $G(z)$ can be described by

$$G_1(z) = \left[\begin{array}{c|c} A_p & B_{pd} \\ \hline C_p & D_{pd} \end{array} \right], G_2(z) = \left[\begin{array}{c|c} A_p & B_p \\ \hline C_p & D_p \end{array} \right] \quad (15)$$

Consider the generic AW configuration shown in figure 3. As illustrated above the plant takes the form $G = [G_1 \; G_2]$, the linear controller is represented by $K = [K_1 \; K_2]$, and $\Theta = [\theta_1 \; \theta_2]$ is the AW controller becoming active only when saturation occurs. Given the difficulty in analyzing the stability and performance of this system we now adopt a framework first introduced in [8] for the problem at hand. This approach reduces to a linear time invariant Anti-Windup scheme that is optimized in terms of one transfer function $M(z)$ shown in figure 4. It was shown in [8] that the performance degradation experienced by the system during saturation is directly related to the mapping $\mathcal{T} : u_{lin} \rightarrow y_d$. Note that from figure 4 $M - I$ is considered for stability of $\mathcal{T}$ and G_2M determines the systems recovery after saturation. This decoupled representation visibly shows how this mapping can be utilized as a performance measure for the AW controller. To quantify this we say that an AW controller is selected such that the $\mathcal{L}_2$-gain, $\|\mathcal{T}\|_{i,2}$, of the operator $\mathcal{T}$

$$\|\mathcal{T}\|_{i,2} = \sup_{0 \neq u_{lin} \in \mathcal{L}_2} \frac{\|y_d\|_2}{\|u_{lin}\|_2}$$

where the $\mathcal{L}_2$ norm $\|x\|_2$ of a discrete signal $x(h), (h = 0, 1, 2, 3, ...)$ is

$$\|x\|_2 = \sqrt{\sum_{h=0}^{\infty} \|x(h)\|^2}$$

A. Static anti-windup synthesis

Static AW has an advantage in that it can be implemented at a much lower computational cost and adds no additional states to the closed loop system. Full order AW synthesis or AW with order equal to the plant will often lead to less response deterioration during saturation, however significant computation is required. This is often unacceptable, especially in systems which are of higher order and where additional states are undesirable. For this reason in practice most windup problems have been suppressed using static compensators, see for example [12]. Using the aforementioned conditioning technique via $M(z)$, outlined in [13], Θ from figure 3 is given by

$$\begin{bmatrix} \theta_1 \\ \theta_2 \end{bmatrix} = \Theta \hat{u} = \begin{bmatrix} \theta_1 \\ \theta_2 \end{bmatrix} \hat{u}$$

u is derived from figure 3 and figure 4 respectively, as

$$u = K_1 r + K_2 y - [(I - K_2 G_2)M - I]\hat{u}$$
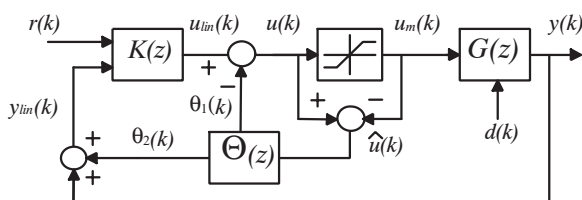
Fig. 3. A generic anti-windup scenario.
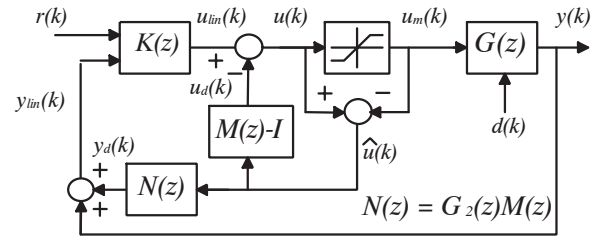
Fig. 4. Weston Postlethwaite Anti-Windup conditioning technique.

$$u = K_1 r + K_2 y + (K_2 \Theta_2 - \Theta_1)\hat{u}$$

Thus $M(z)$ can be written as

$$M = (I - K_2 G_2)^{-1}(-K_2\Theta_2 + \Theta_1 + I)$$

The goal of the static AW approach is therefore to ensure that extra modes do not appear in the system. Since this will inevitably be the case it must be ensured that minimal realizations of the controller and plant are used [9]. A state space realization can then be formed

$$\begin{bmatrix} M(z) - I \\ N(z) \end{bmatrix} \sim \begin{bmatrix} \dot{\bar{x}} \\ u_d \\ y_d \end{bmatrix} = \begin{bmatrix} \bar{A} & B_0 + \bar{B}\Theta \\ \hline C_1 & D_{01} + D_1\Theta \\ \bar{C}_2 & D_{02} + \bar{D}_2\Theta \end{bmatrix} \begin{bmatrix} \bar{x} \\ \hat{u} \end{bmatrix}$$

(16)

where $\Theta = [\Theta_1' \Theta_2']'$ is a static matrix and $\bar{x}$, $\bar{A}$, B_0, $\bar{B}$, $\bar{C}_1$, D_{01}, $\bar{D}_1$, $\bar{C}_2$, D_{02} and $\bar{D}_2$ are minimal realizations given in [9].

In a similar manner to [14] a solution is obtained for the LMI

$$\begin{bmatrix} -Q & -Q\bar{C}_1' & Q\bar{A}' & 0 & Q\bar{C}_2' \\ - & -X & UB_0 + L'\bar{B}' & I & UD_{02}' + L'\bar{D}_2' \\ - & - & -Q & 0 & 0 \\ - & - & - & -\gamma I & 0 \\ - & - & - & - & -\gamma I \end{bmatrix} < 0$$

(17)

Where $X = 2U + D_{01}U + \bar{D}_1 L + UD_{01}' + L'\bar{D}_1'$ and with $Q > 0$, $U = diag(v_1, ...v_c) > 0$, $L \in \Re^{(c+n) \times n}$ (where $c = n$), and the minimized $\mathcal{L}_2$ gain $\|\mathcal{T}\|_{i,2} < \gamma$ (where γ is the $\mathcal{L}_2$ gain bound on $\mathcal{T}$). In this instance Θ is given by $\Theta = LQ^{-1}$ using which the controller in 16 can be synthesized. This $\mathcal{L}_2$ design ensures that during saturation closed loop performance is achieved by staying close to the nominal design while the time spent in saturation is also jointly minimized. Applying this synthesis routine to our plant given by (4) and linear controller (13), the resultant controller is $\Theta = [-0.2049 \; 0.6377]'$ obtained using the LMI toolbox in Matlab[1].

V. PRACTICAL IMPLEMENTATION AND DISCUSSION

A. Testbed Description and Performance Criteria

The Tmote Sky mote sensor node is an embedded platform using an 802.15.4 compliant transceiver and is selected as the primary embedded platform for this work. Tmote's

[1]The Mathworks Inc.

Fig. 5.   802.15.4 Wireless experimental scenario.

transceiver the CC2420 provides an RSSI measurement in dBm by averaging the received signal power over 8 symbol periods or $128\mu s$. An interface between Matlab and TinyOS has been established using TinyOS Matlab tools written in Java [15]. Sensor data packets are framed in 802.15.4 format and transmitted using the TinyOS library function Oscope. The base station bridges packets over the USB/Serial connection to a personal computer. The Matlab application identifies the connection by its phoenixSource name e.g. 'network@localhost:9000' or by its serial port name e.g. 'serial@COM3:tmote' and imports the packets directly into the Matlab environment.

The experimental setup shown in figure 5, consists of a five Tmote nodes and one additional Tmote acting as a base station. Three fully autonomous MIABOT Pro [16] miniature mobile robots are used to introduce mobility into the system and can be removed and reintroduced as necessary. Each of the control strategies to be examined is rigorously tested using this scenario. Initially all five nodes are stationary and the experiment is executed five times for five randomly selected node positions. The experiment is 200(sec) in duration. One mobile node is then introduced to the system and the scenario is repeated again for 5 randomly chosen positions for the remaining 4 stationary nodes. A second and finally a third mobile is introduced and the scenario is repeated. Each strategy is therefore evaluated for a total of 20 experiments, spending over an hour in operation and with varied levels of mobility within the system. For consistency the trajectories along which the mobile robots move remain the same for each experiment.

A sampling frequency of $T_s = 3(sec)$ is used throughout and a target RSSI value of -55dBm is selected for tracking, guaranteeing a PER of $< 1\%$, verified using equations (5), (6) and (7). The standard deviation of the RSSI tracking error is chosen as a performance criterion:

$$\sigma_e = \left\{ \frac{1}{S} \sum_{k=1}^{S} [r(k) - RSSI(k)]^2 \right\}^{\frac{1}{2}} \qquad (18)$$

where S is the total number of samples and k is the index of these samples. Outage probability is defined as

$$P_o(\%) = \frac{number\ of\ times\ RSSI\ <\ RSSI_{th}}{the\ total\ number\ of\ iterations} \times 100 \qquad (19)$$

where $RSSI_{th}$ is selected to be -57dBm, a value below which performance is deemed unacceptable in terms of PER. This can be easily verified again using equations (5), (6) and (7). To fully access each paradigm, some measure of power efficiency is also useful and here we define average power consumption as the average power consumed by all motes operating using a particular power control algorithm for the duration of an experiment. Therefore given there are five motes in the cell we calculate the power consumption by firstly averaging the power consumed throughout the experiment on an individual basis and then the average of these five values gives us the overall average power consumption.

B. Benchmark Comparative Study

In this section the performance of the WPAW Static controller is compared with fixed step [17], H∞/LMI [4] and adaptive step [18] active power control methods. Figure 6(b) illustrates how the proposed hybrid system performs when compared to the approaches outlined above. Clearly the hybrid design outperforms the adaptive approach for all of the criteria and shows substantial improvement over the conventional/H∞ in terms of standard deviation and outage probability with low mobility in the system. However with fewer mobile nodes in the system the conventional/H∞ approach consumes less power. This is as a result of the aggressive response of the pre-filter and is worthwhile when the improved tracking performance is considered. As the number of mobile users is increased the standard deviations of the hybrid design and the conventional/H∞ converge, however the hybrid design continues to exhibit improved outage probability. The average power consumptions of the two approaches also converge, highlighting improved power efficiency characteristics for the hybrid design with increased mobility. This is to be expected given AW inherently seeks to decrease the magnitude of the controller output.

VI. CONCLUDING REMARKS

To conclude, power control in wireless networks where operational longevity is paramount can be very useful, however it can also be used to provide pre-specified levels of quality of service. It is therefore important to consider both power efficiency and link estimation when deciding upon or designing a power control paradigm. This work does both in that it selects a priori, a level of performance in terms of packet error rate, attainable using minimum power. The hybrid controller designed and practically tested to achieve this, considers both robust stability (disturbance rejection) and performance (tracking) within its linear design and also considers communication constraints using a conservative anti-windup scheme. The results of extensive testing summarized in table 1, show how accounting for the presence of
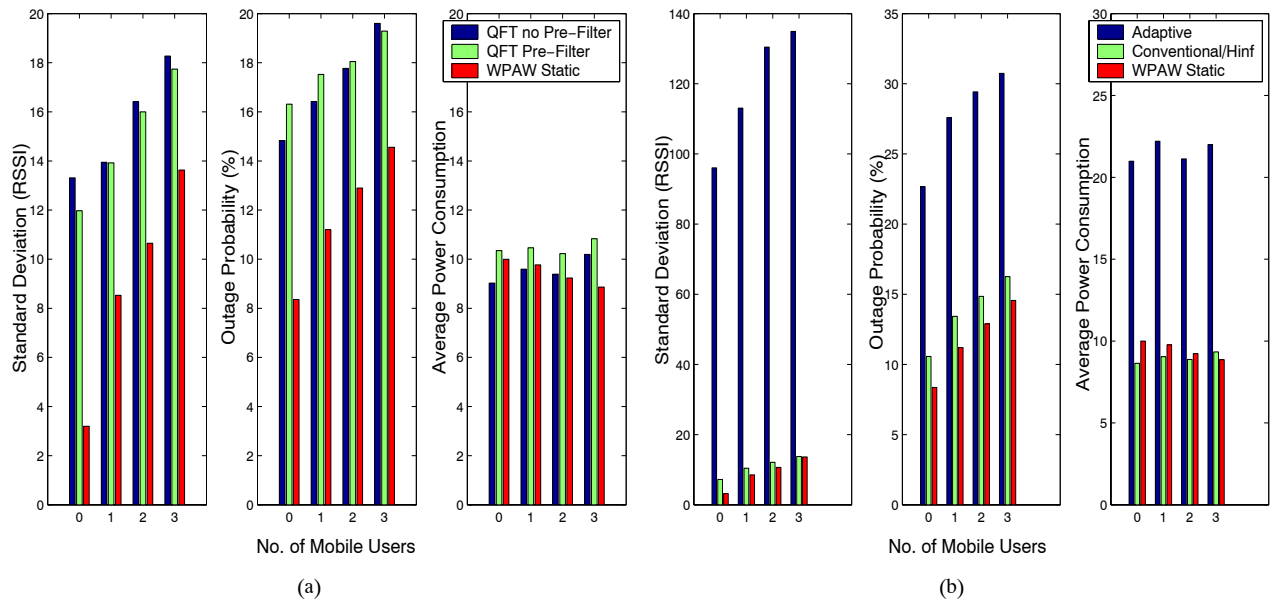
Fig. 6. (a) Comparison with and without pre-filter and with and without AW and (b) Comparison between adaptive, conventional/H∞ and WPAW Static approaches.

TABLE I

CHARACTERISTICS: σ_e - STANDARD DEVIATION, P_o - OUTAGE PROBABILITY, P_{av} - AVERAGE POWER CONSUMPTION

No. of Mobiles	Adaptive			Conventional/ LMI			QFT without Pre-Filter			QFT with Pre-Filter			Hybrid QFT/ Static AW		
	σ_e	P_o	P_{av}	σ_e	P_o	P_{av}	σ_e	P_o	P_{av}	σ_e	P_o	P_{av}	σ_e	P_o	P_{av}
0	96	22.7	20.9	7.2	10.6	8.6	13.3	14.8	9	12	16.3	10.4	3.1	8.3	9.9
1	113	27.6	22.2	10.4	13.4	9	13.9	16.4	9.6	14	17.5	10.5	8.5	11.2	9.7
2	130.4	29.4	21.1	12.1	14.8	8.9	16.4	17.8	9.4	16	18	10.2	10.6	12.8	9.2
3	134.9	30.7	21.9	13.7	16.2	9.3	18.3	19.6	10.2	17.7	19.2	10.8	13.6	14.5	8.8

static memory-less nonlinearities can dramatically improve overall system performance.

REFERENCES

[1] B. Zurita Ares, C. Fischione, A. Speranzon, and K. H. Johansson. On power control for wireless sensor networks: system model, middleware component and experimental evaluation. *European Control Conference*, Kos, Greece, 2007.

[2] K. Srinivasan and P. Levis, RSSI is Under Appreciated, *Third Workshop on Embedded Networked Sensors (EmNets)*, 2006

[3] IEEE Standard, Wireless lan medium access control (mac) and physical layer (phy) specifications for low-rate wireless personal area networks (lr-wpans), IEEE Std 802.15.4 (2006).

[4] Yuan-Ho Chen Bore-Kuen Lee and Bor-Sen Chen, Robust Hinf Power Control for CDMA Cellular Communication Systems, *IEEE Transactions on Signal Processing*, 2006, (54)(10): 3947–3956.

[5] A. Subramanian and A. H. Sayed, Joint rate and power control algorithms for wireless networks, *IEEE trans. sig. process.*, 2005, (53)(11): 42044214.

[6] M. Turner, G. Herrmann and I. Postlethwaite, Incorporating robustness requirements into anti-windup design, *IEEE Transactions on Automatic Control*, 2007, (52)(10): 1842-1855.

[7] D.S. Bernstein and A.N. Michel, A chronological bibliography on saturating actuators, *International Journal of Robust and Nonlinear Control*, 1995, (5): 375-380.

[8] P.F. Weston and I. Postlewaite, Analysis and design of linear conditioning schemes for systems containing saturating actuators, *Proc. IFAC Nonlinear Control System Design Symp*, 1998.

[9] G. Herrmann, M. Turner and I. Postlethwaite, Discrete-time and sampled-data anti-windup synthesis: stability and performance, *International Journal of Systems Science*, 2006, (37)(2): 91-114.

[10] I. Horowitz, Survey of quantitative feedback theory (QFT), *Int. J. Robust Nonlinear Control*, Vol. 11, 2001, pp. 887–921.

[11] C. Borghesani, Y. Chait, and O. Yaniv, *The QFT Frequency Domain Control Design Toolbox For Use with MATLAB*, Terasoft, Inc., 2003.

[12] R. Hanus, M. Kinnaert and J. Henrotte, Conditioning technique a general anti-windup and bumpless transfer method, *Automatica*, 1987, (23): 729-39.

[13] M. Turner and I. Postlethwaite, A new perspective on static and low-order anti-windup synthesis, *International Journal of Control*, 2004, (77): 27-44.

[14] G. Herrmann, M.C. Turner, I. Postlethwaite and G. Guo, Practical Implementation of a Novel Anti- Windup Scheme in a HDD-Dual-Stage Servo-System, *IEEE/ASME Transactions on Mechatronics*, 2004, (9)(3).

[15] M. Walsh, M. Hayes, and J. Nelson, Robust Performance for an Energy Sensitive Wireless Body Area Network - An Anti-Windup Approach,*International Journal of Control*, Accepted for publication, 2008.

[16] MIABOT Pro fully autonomous miniature mobile robot. http://www.merlinrobotics.co.uk/merlinrobotics/, [January 10, 2008]

[17] F. Gunnarsson, F. Gustafsson, and J. Blom, Pole placement design of power control algorithms, *In Proc. IEEE Vehicular Technology Conference*, Houston, TX, USA, May 1999.

[18] A. Goldsmith, *Wireless Communications*, Cambridge University Press; 2006.